

## Three-dimensional modeling of electron quasiviscous dissipation in guide-field magnetic reconnection

Michael Hesse, Masha Kuznetsova, Karl Schindler, and Joachim Birn

Citation: *Physics of Plasmas* (1994-present) **12**, 100704 (2005); doi: 10.1063/1.2114350

View online: <http://dx.doi.org/10.1063/1.2114350>

View Table of Contents: <http://scitation.aip.org/content/aip/journal/pop/12/10?ver=pdfcov>

Published by the [AIP Publishing](#)

---

### Articles you may be interested in

[Three-dimensional model and simulation of vacuum arcs under axial magnetic fields](#)

*Phys. Plasmas* **19**, 013507 (2012); 10.1063/1.3677881

[Model of electron pressure anisotropy in the electron diffusion region of collisionless magnetic reconnection](#)

*Phys. Plasmas* **17**, 122102 (2010); 10.1063/1.3521576

[Onset and saturation of guide-field magnetic reconnection](#)

*Phys. Plasmas* **12**, 062301 (2005); 10.1063/1.1914309

[The role of electron heat flux in guide-field magnetic reconnection](#)

*Phys. Plasmas* **11**, 5387 (2004); 10.1063/1.1795991

[Computer studies on the three-dimensional spontaneous fast reconnection model as a nonlinear instability](#)

*Phys. Plasmas* **11**, 1416 (2004); 10.1063/1.1677110

---



### Vacuum Solutions from a Single Source

- Turbopumps
- Backing pumps
- Leak detectors
- Measurement and analysis equipment
- Chambers and components

**PFEIFFER**  **VACUUM**

## Three-dimensional modeling of electron quasiviscous dissipation in guide-field magnetic reconnection

Michael Hesse and Masha Kuznetsova

National Aeronautics and Space Administration (NASA) Goddard Space Flight Center, Greenbelt, Maryland 20771

Karl Schindler

Ruhr-Universität, 44780 Bochum, Germany

Joachim Birn

Los Alamos National Laboratory, Los Alamos, New Mexico 87545

(Received 19 August 2005; accepted 19 September 2005; published online 24 October 2005)

A numerical study of guide-field magnetic reconnection in a three-dimensional model is presented. Starting from an initial, perturbed, force-free current sheet, it is shown that reconnection develops to an almost translationally invariant state, where magnetic perturbations are aligned primarily along the main current flow direction. An analysis of guide-field and electron flow signatures indicates behavior that is very similar to earlier, albeit not three-dimensional, simulations. Furthermore, a detailed investigation of electron pressure nongyrotropies in the central diffusion region confirms the major role the associated dissipation process plays in establishing the reconnection electric field. © 2005 American Institute of Physics. [DOI: 10.1063/1.2114350]

While it now appears that electron quasiviscous dissipation is the likely prime mechanism for establishing a reconnection electric field in antiparallel reconnection geometries,<sup>1–5</sup> there is considerably more debate regarding the mode of operation of the inner electron diffusion region when a finite guide magnetic field is present. Candidate processes here are electron nongyrotropies generated by electron Larmor radius scales of magnetic-field gradients,<sup>6–8</sup> instabilities generated by fast electron beams, such as Buneman modes,<sup>9</sup> or electron inertial processes in very thin electron current layers.<sup>10</sup>

Whichever the process, it is clear that, on a microscopic level, it needs to provide a finite contribution to the electric field (in standard notation),

$$\mathbf{E} = -\mathbf{v}_e \times \mathbf{B} - \frac{1}{n_e e} \nabla \cdot \mathbf{P}_e - \frac{m_e}{e} \left( \frac{\partial \mathbf{v}_e}{\partial t} + \mathbf{v}_e \cdot \nabla \mathbf{v}_e \right), \quad (1)$$

at the reconnection site. If we assume current flow and guide magnetic field to be in the  $y$  direction, (1) is evaluated in the electron diffusion region to yield

$$E_{\parallel} = E_y|_{X \text{ point}} = -\frac{1}{n_e e} \left( \frac{\partial P_{xye}}{\partial x} + \frac{\partial P_{yye}}{\partial y} + \frac{\partial P_{yze}}{\partial z} \right) - \frac{m_e}{e} \left( \frac{\partial v_{ey}}{\partial t} + \mathbf{v}_e \cdot \nabla v_{ey} \right). \quad (2)$$

As is evident from (2), the parallel electric field has to be related to thermal inertia terms (the divergence of the electron pressure tensor), or bulk inertia terms with temporal or spatial derivatives of the electron bulk flow speed.

In nonrelativistic applications, the time derivative on the right-hand side of (2) usually remains ignorable.<sup>7</sup> In order to study the relevance of the remaining terms, it is necessary to perform high-resolution numerical simulations with sufficiently large particle numbers to resolve scales as small as

electron Larmor radii, and small electron nongyrotropies.<sup>7</sup> In this paper, we present the first results of such three-dimensional simulations, with the goal to specifically resolve all relevant spatial scales and where a substantially large particle number was employed in order to reduce the inevitable noise in three-dimensional particle-in-cell simulations.

Throughout this paper, we will utilize dimensionless quantities. For this purpose, we normalize densities by a typical density  $n_0$ , and the magnetic field by the asymptotic value of the reconnecting magnetic field  $B_0$ . Length scales are normalized by the ion inertial length  $c/\omega_i$ , where the ion plasma frequency  $\omega_i = \sqrt{e^2 n_0 / \epsilon_0 m_p}$  is evaluated for the reference density  $n_0$ . Velocities are measured in units of the ion Alfvén velocity  $v_A = B_0 / \sqrt{\mu_0 m_p n_0}$ . The electric field is measured in units of  $E_0 = v_A B_0$ , the pressure in units of  $p_0 = B_0^2 / \mu_0$ , and the current density is normalized to  $j_0 = \omega_i B_0 / c \mu_0$ . Time is expressed in units of ion cyclotron periods.

In order to avoid unrealistic growth behaviors for the mass ratio employed here of kink<sup>11,12</sup> and lower hybrid drift<sup>13–15</sup> (LHD) modes for the mass ratio employed here (see below), we utilize as an initial condition a perturbed force-free current sheet. We emphasize that both LHD and kink modes are known to modify the current sheet profile.<sup>13,15</sup> However, in a three-dimensional calculation, it is not feasible to reproduce this behavior correctly. The poloidal magnetic field is of the form

$$B_x = \tanh(z/l) + a_0 \pi / L_z \cos(2\pi x / L_x) \sin(\pi z / L_z), \quad (3)$$

$$B_z = -a_0 2\pi / L_z \sin(2\pi x / L_x) \cos(\pi z / L_z), \quad (4)$$

whereas the toroidal magnetic field fulfills

$$B_y = \sqrt{(\cosh(z/l))^{-2} + B_{y0}^2} - a_0 2\pi/L_z \sin(2\pi x/L_x) \cos(\pi z/L_z). \quad (5)$$

We choose  $B_{y0}=0.8$  as the asymptotic value of the guide field. The initial density and pressure distributions are homogeneous with magnitudes of unity and 0.5, respectively, and the current density is initially supported by the electrons alone. In order to obtain a rapid reconnection initiation, the initial current sheet full width is selected to be  $2l=0.7$ . The perturbation amplitude  $a_0=0.1$  leads to an initial value of the normal magnetic field of about 3% of  $B_0$ . The system sizes are  $L_x=13.9$ ,  $L_y=8.5$ , and  $L_z=6.9$ . The time step is  $\omega_e dt=1$ , and energy is conserved to within a few percent throughout the run.

The ion-electron mass ratio is chosen to be  $m_i/m_e=50$ . A total of  $1 \times 10^9$  macroparticles are employed during the calculation, and an electron/ion temperature ratio of  $T_e/T_i=0.2$  has been adopted. The system evolution is modeled by our particle-in-cell code<sup>3,7</sup> on a grid composed of  $171 \times 101 \times 171$  cells in the  $x$ ,  $y$ , and  $z$  directions, respectively. Periodic boundary conditions are employed in the  $x$  and  $y$  directions, whereas the particles are specularly reflected at the upper and lower boundaries.

The initial condition, as described by Eqs. (3)–(5), describes a perturbed magnetohydrodynamic equilibrium, but only an approximate kinetic equilibrium. The deviations from kinetic equilibrium manifest themselves in fluctuations that initially grow outside the current sheet and subsequently propagate into the current sheet region. Consequently, the evolution prior to  $t=8$  is dominated by these initial fluctuations. While these fluctuations may lead to the onset of reconnection, we are primarily interested in the nonlinear evolution of reconnection. We will therefore focus on the evolution thereafter.

Figure 1 shows the magnetic field normal to the current sheet plane ( $B_z$ ) during three different times ( $t=9, 15, 20$ ) of the subsequent evolution. The initial, highly structured perturbation begins to self-organize before  $t=9$ , and has reached an almost  $y$ -independent state by  $t=15$  and thereafter. The formation of elongated reconnection channels has been seen before in simulations of antiparallel<sup>16</sup> and guide-field magnetic reconnections.<sup>17</sup>

The formation of the reconnection channels is associated with the fast transport of newly reconnected magnetic flux in the direction of the electron flow. Outside the immediate electron diffusion region, the magnetic field is frozen into the electron flow. The electron flow near the electron diffusion region is dominated by the presence of a very thin electron current sheet (see below), such that electrons move rapidly into the negative  $y$  direction. This motion implies that newly generated magnetic flux normal to the current sheet will get swept along by the electron flow, thereby generating patterns elongated in the  $y$  direction. This mechanism is similar to findings for antiparallel reconnection.<sup>16,18</sup>

Figure 2 displays the evolution in time of the total amount of the reconnected magnetic flux

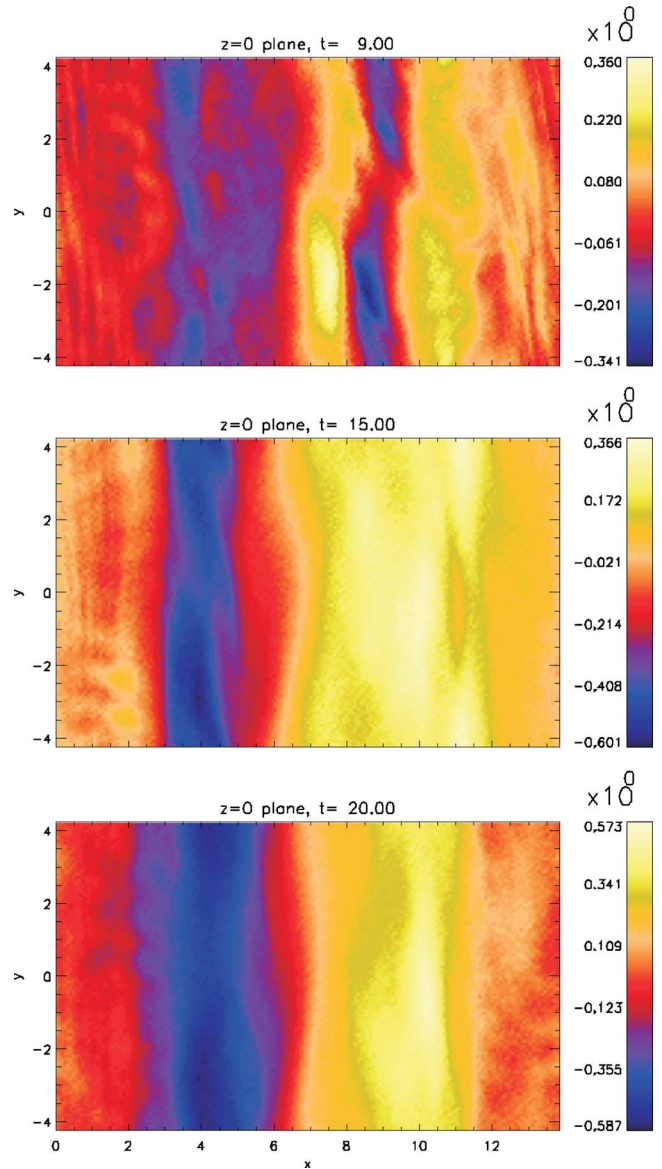


FIG. 1. (Color online). Normal magnetic-field component  $B_z$  in the current sheet plane for three different times of the simulation. The panels show a self-organization of the reconnection process from a number of substructures to an elongated reconnection channel.

$$\Phi = \int_{B_z > 0} B_z(z=0) dx dy \quad (6)$$

as well as an estimate of the average reconnection electric field  $E_r$ , derived by

$$\frac{\partial \Phi}{\partial t} = E_r L_y. \quad (7)$$

The overall reconnection rate is only slightly smaller than the rates found in translationally invariant models<sup>6–8</sup> and than the rates in antiparallel reconnection models,<sup>19</sup> despite the higher overall density and the presence of the guide magnetic field.

A more detailed analysis of the central ( $y=0$ ) plane is presented in Fig. 3. The upper panel displays the structure of the guide magnetic field ( $B_y$ ) component. The bottom panel

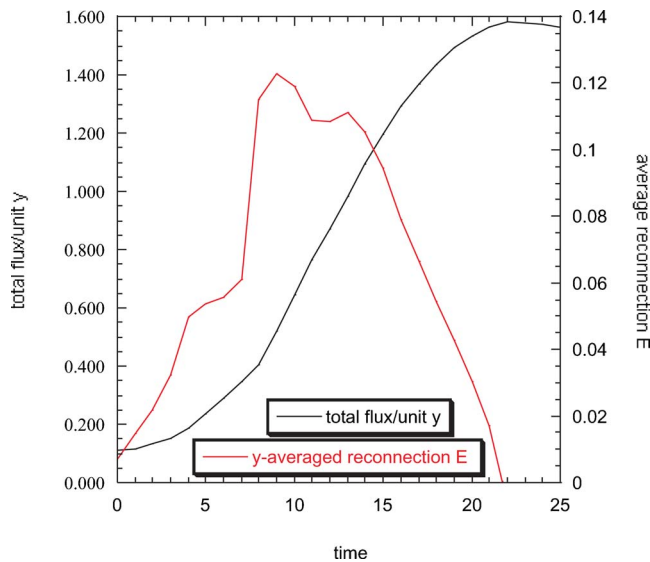


FIG. 2. (Color online). Growth of the integrated  $B_z$  perturbation (reconnected flux) in the current sheet plane and average reconnection electric field.

of Fig. 3 depicts the variation of the electron current density in the same plane. The panel demonstrates the presence of a very strong and localized electron current sheet in the electron diffusion region, with weaker branches extending along one edge of the  $B_y$  enhancement regions. Overall, the  $B_y$  modulation and the electron current sheet appear to be morphologically rather similar to results from translationally invariant models.

A final comparison focuses on the dissipation mechanism. While 2.5-dimensional models predict a comparatively laminar, thermal inertia-based dissipation process, it is pos-

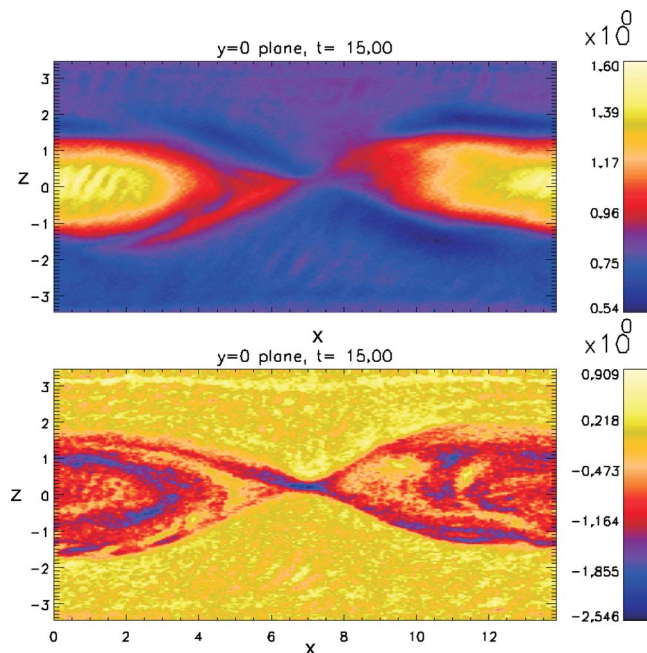


FIG. 3. (Color online). Variation in the  $y=0$  plane, of the magnetic guide-field component  $B_y$  (top panel), and of the electron current density  $j_y$  (bottom panel), for time  $t=15$ .

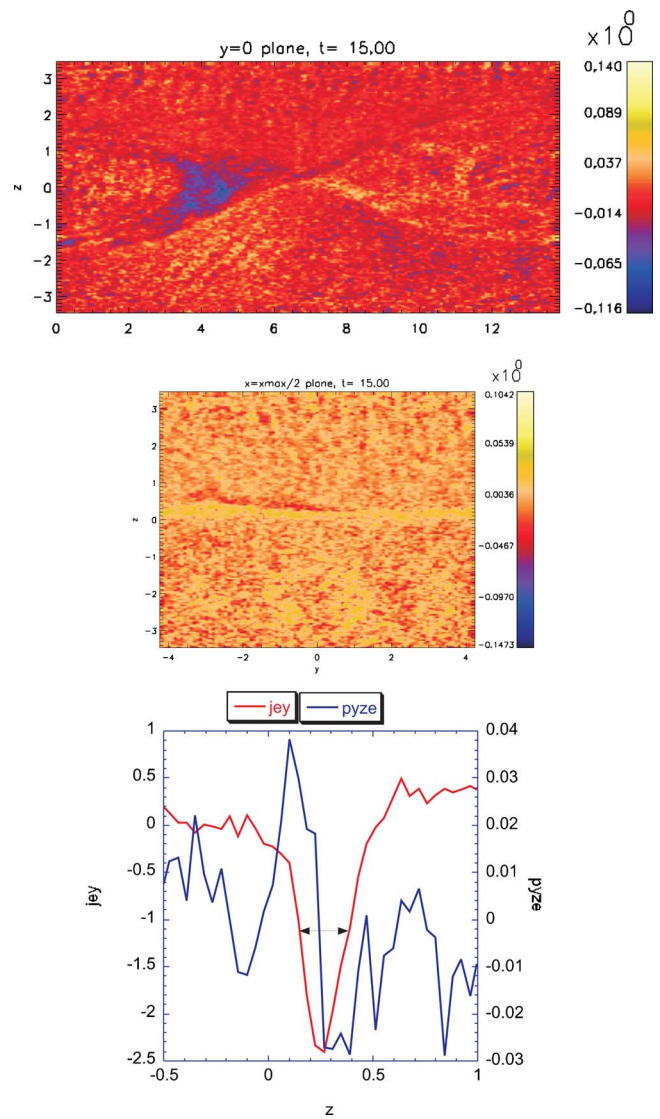


FIG. 4. (Color online). Electron pressure tensor component  $P_{yze}$  in the  $y=0$  plane (top panel) and in the  $x=6.9$  plane (bottom panel). The bottom panel shows a plot, along  $z$ , of the electron current density and of  $P_{yze}$  at  $x=6.9$  and  $y=-0.47$ , together with the electron Larmor orbit diameter (black double arrow). All panels are for  $t=15$ .

sible that turbulence in a fully three-dimensional model may lead to strong spatiotemporal fluctuations. While the latter will, on a microphysical level, also be represented by a combination of thermal and bulk inertia effects (2), it may be very difficult to analyze pressure tensors and bulk inertia terms under these conditions. The question is which route the system chooses if it is left to its own devices.

Figure 4 answers this question for the later times of the present calculation. From previous work, we expect the electron pressure tensor component  $P_{yze}$  to play the dominant role in (2) in the absence of turbulence.<sup>7</sup> The top two panels of Fig. 4 display this component in two different planes, the central,  $y=0$ , plane (top panel), and in a perpendicular cut along the main current direction, in the  $x=6.9$  plane. No smoothing has been applied to this direct derivation from particle data. These two panels display a clear positive-

negative variation for ascending  $z$ , centered about the electron current sheet location.

A more detailed analysis is shown in the bottom panel of Fig. 4, which presents a cut along the  $z$  direction, located at  $x=6.9$  and  $y=-0.47$ . The graphs show the variation of the  $P_{yze}$  pressure tensor component along with that of the electron current density. The black double arrow indicated the local electron Larmor orbit diameter. The electron pressure variations are located at the edge of the current density peak. The length scale for both current and pressure tensor nongyrotropies is associated with the electron Larmor radius.

The typical density in this region is  $n_e=0.9$ . Using, from the figure, a pressure variation of  $\Delta P_{yze}=-0.06$ , we can derive an approximate reconnection electric field, at this location by using (2),

$$E_r \approx -\frac{1}{en_e} \frac{\Delta P_{yze}}{\Delta z} \approx 0.17. \quad (8)$$

All other derivatives in Eq. (2) are negligible. This value is only slightly larger than the overall rates shown in Fig. 2, indicating that there are small variations of the reconnection rate along the channel shown in Fig. 1. The result does show, however, that the pressure tensor-derived electric field can supply the dominant contribution to the reconnection electric field even in a fully three-dimensional simulation.

In summary, this study employed fully three-dimensional electromagnetic particle-in-cell simulations to study the electron dissipation region of collisionless magnetic reconnection. The main goal of the study was to investigate whether the electron quasiviscous dissipation mechanism<sup>1-3,7</sup> also applies in a fully three-dimensional environment, where additional degrees of freedom open up the possibility for additional avenues of dissipation mechanisms. Based on the expected properties of electron quasiviscous dissipation, we set up the simulation such that the model resolves the local electron Larmor radius in the dissipation region.

In order to avoid unrealistic growth of modes such as the lower-hybrid drift instability,<sup>13-15</sup> we chose as an initial condition a perturbed, force-free, fluid equilibrium with an initially spatially constant density and pressure. The trade-off proved to be an initial adjustment phase, which is likely driven by the lack of kinetic equilibrium of the initial fluid equilibrium. The fluctuations associated with this adjustment originated well outside the current sheet, and subsequently preceded into the current sheet proper. Therefore, a study of

the initial evolution of the simulation was outside the scope of this investigation.

After the adjustment period, however, the calculation featured the establishment of pronounced reconnection channels elongated along the main current direction. A detailed analysis of this reconnections channel revealed a structure very similar to that seen in earlier high-resolution, translationally invariant models.<sup>7</sup> These results include the dominance of the electron quasiviscous dissipation, which readily provided the required magnitude of the reconnection electric field.

Therefore, the present research shows that electron quasiviscous dissipation remains a viable dissipation process even if the dynamics is not constrained to variations in two spatial dimensions only. The question whether this dissipation process is dominant in all possible situations or not, however, will provide topics for challenging and intriguing future investigations.

This research was supported by NASA's Sun-Earth Connection Theory Program (SECTP). We appreciate stimulating discussions with J. Drake and Phil Pritchett.

<sup>1</sup>R. Horiuchi and T. Sato, Phys. Plasmas **1**, 3587 (1994).

<sup>2</sup>M. Hesse and D. Winske, J. Geophys. Res. **99**, 11177 (1994).

<sup>3</sup>M. Hesse, K. Schindler, J. Birn, and M. Kuznetsova, Phys. Plasmas **6**, 1781 (1999).

<sup>4</sup>P. Ricci, G. Lapenta, and J. U. Brackbill, Geophys. Res. Lett. **29**, 2088 (2002).

<sup>5</sup>P. L. Pritchett, J. Geophys. Res. **106**, 25961 (2001).

<sup>6</sup>P. Ricci, J. U. Brackbill, W. Daughton, and G. Lapenta, Phys. Plasmas **11**, 4102 (2004).

<sup>7</sup>M. Hesse, M. Kuznetsova, and J. Birn, Phys. Plasmas **11**, 5387 (2004).

<sup>8</sup>P. L. Pritchett, Phys. Plasmas **12**, 062301 (2005).

<sup>9</sup>J. F. Drake, M. Swisdak, C. Cattell, M. A. Shay, B. N. Rogers, and A. Zeiler, Science **299**, 873 (2003).

<sup>10</sup>P. L. Pritchett and F. V. Coroniti, J. Geophys. Res. **109**, 1220 (2003).

<sup>11</sup>W. Daughton, J. Geophys. Res. **104**, 28701 (1999).

<sup>12</sup>M. Hesse and J. Birn, in *Magnetospheric Current Systems*, Geophysical Monograph Series Vol. 118, edited by S. Ohtani, R. Fujii, M. Hesse, and R. Lysak (AGU, Washington, DC, 2000), p. 295.

<sup>13</sup>W. Daughton, Phys. Plasmas **9**, 3668 (2002).

<sup>14</sup>W. Daughton, Phys. Plasmas **10**, 3103 (2003).

<sup>15</sup>W. Daughton, G. Lapenta, and P. Ricci, Phys. Rev. Lett. **93**, 105004 (2004).

<sup>16</sup>M. Hesse, M. Kuznetsova, and J. Birn, J. Geophys. Res. **106**, 29831 (2001).

<sup>17</sup>M. Scholer, I. Sidorenko, C. H. Jaroscheck, R. A. Treumann, and A. Zeiler, Phys. Plasmas **10**, 3521 (2003).

<sup>18</sup>J. D. Huba and L. I. Rudakov, Phys. Rev. Lett. **93**, 175003 (2004).

<sup>19</sup>J. Birn, J. F. Drake, M. A. Shay, B. N. Rogers, R. E. Denton, M. Hesse, M. Kuznetsova, Z. W. Ma, A. Bhattacharjee, A. Otto, and P. L. Pritchett, J. Geophys. Res. **106**, 3715 (2001).